Chemistry & Biology
Article

Substrate-Dependent Targeting of Eukaryotic Translation Initiation Factor 4A by Pateamine A: Negation of Domain-Linker Regulation of Activity

Woon-Kai Low,[1] Yongjun Dang,[1] Shridhar Bhat,[1] Daniel Romo,[2] and Jun O. Liu[1,3,4,*]
[1] Department of Pharmacology and Molecular Sciences, Johns Hopkins School of Medicine, Baltimore, MD 21205, USA
[2] Department of Chemistry, Texas A&M University, College Station, TX 77842, USA
[3] Solomon H. Snyder Department of Neuroscience
[4] Department of Oncology
Johns Hopkins School of Medicine, Baltimore, MD 21205, USA
*Correspondence: joliu@jhu.edu
DOI 10.1016/j.chembiol.2007.05.012

SUMMARY

Central to cap-dependent eukaryotic translation initiation is the eIF4F complex, which is composed of the three eukaryotic initiation factors eIF4E, eIF4G, and eIF4A. eIF4A is an RNA-dependent ATPase and an ATP-dependent helicase that unwinds local secondary structure in mRNA to allow binding of the 43S ribosomal complex. The marine natural product pateamine A (PatA) has been demonstrated to inhibit cap-dependent initiation by targeting eIF4A and disrupting its protein-protein interactions while increasing its enzymatic activities. Here we demonstrate that the increased activity is caused by the induction of global conformational changes within eIF4A. Furthermore, binding of PatA is dependent on substrate (RNA and ATP) binding, and the increased activity upon PatA binding is caused by relief of a negative regulatory function of the eIF4A unique domain linker.

INTRODUCTION

Proteins of the DEAD box (DDX) family are defined by the presence of nine conserved motifs, belong to helicase superfamily II (SF2), and are involved in a myriad of cellular processes [1–4]. The core of SF2 proteins consists of two tandemly repeated RecA-like domains. Motifs I (Walker A), Ia, Ib, II (Walker B with the sequence D-E-A-D, for which the family is named), III, and Q are found in the N-terminal domain, and motifs IV, V, and VI are found in the C-terminal domain. The founding member, and prototypical DDX protein, eukaryotic translation initiation factor 4A (eIF4A) consists only of the two domains [4–6]. In humans, there are three forms of eIF4A: I (DDX2A) and II (DDX2B), which are 90% identical and functionally equivalent although they are differentially regulated in cell growth [7], and III (DDX48), which is ~65% identical to I. eIF4A possesses RNA-dependent ATPase and nonprocessive ATP-dependent helicase activity [6]. eIF4AI and II function in translation initiation [8, 9], whereas eIF4AIII, along with proteins MLN51, Magoh, and Y14, forms the core of the exon junction complex (EJC), which is deposited ~20–24 nt upstream from exon-exon splicing sites [10].

In translation initiation, eIF4AI is the most abundant of the translation initiation factors and is found in free form, with approximately 10% of the total eIF4AI in complex with eIF4E and eIF4G [8, 9, 11]. Together, eIF4E, eIF4G, and eIF4A are known as eIF4F, which is believed to recruit 43S ribosomal particles (40S ribosomal subunit primed for translation and bound by eIF3 and the eIF2-GTP-Met-tRNA$_i$ ternary complex) to m^{7}GTP-capped eukaryotic mRNA through interactions of the cap with eIF4E and interactions between eIF4G and eIF3 [8, 9, 12]. Current models suggest that eIF4A's role is to unwind small regions of local secondary structure within the mRNA to allow binding of the 43S complex [13]. Furthermore, this process is proposed to be enhanced by eIF4B, a protein known to increase both the processivity of eIF4AI helicase activity and ATPase activity [14–16], and eIF4F-bound eIF4A has been proposed to be in active exchange with the free form during initiation [11, 17].

Structural determinations of DDX proteins have demonstrated a shared topology with well-conserved folds within the individual RecA-like domains; however, the orientations of the two domains with respect to each other vary significantly between different proteins [2, 5]. Crystallographic studies of the yeast eIF4AI homolog tif1p demonstrated a "dumbbell-like" structure, with the two domains separated by a flexible linker [18]. Previous studies using limited proteolysis have demonstrated a cycle of conformational changes associated with ATP and RNA binding, and with hydrolysis of ATP to ADP acting to modulate RNA affinity [19, 20]. More recent crystallographic studies of eIF4A homologs in the presence of substrates AMP-PNP, nonhydrolyzable ATP analog, and RNA have demonstrated conformational changes within the domain linker that allow for the close proximity of the two domains required for enzymatic activity [21–23].

Recently, the small marine natural product pateamine A (PatA) [24] has been identified as an inhibitor of eukaryotic translation initiation by directly targeting eIF4AI and II, leading to formation of stress granules at the cellular level

[25–28]. PatA-affinity resin was also demonstrated to capture eIF4AIII [28]. Furthermore, the simplified derivative *des*-methyl, *des*-amino pateamine A (DMDA-PatA) [29] was demonstrated to act by a similar mechanism to PatA with only slightly less potency [26]. Surprisingly, PatA was found to increase both the ATPase and helicase activities of eIF4AI with increased affinities for both ATP and RNA [26, 28], and initial evidence suggested that PatA may perturb the normal protein-protein interactions of eIF4A by decreasing association with eIF4G and increasing association with eIF4B [26]. In this work, we have further characterized the functional impact of PatA on eIF4AI. We have demonstrated the minimal requirement for RNA to induce global conformational changes and the need for both AMP-PNP and RNA for tight binding of the biotin-conjugated PatA analog (B-PatA) to eIF4A. PatA induced a more "closed" conformation, and the increased activity induced by PatA likely arises by relieving inhibitory effects of the eIF4AI-, II-, and III-specific domain-linker sequence.

RESULTS

Stabilization of 6×His-eIF4AI with Respect to Trypsin Proteolysis in the Presence of DMDA-PatA

The cycle of conformational changes for eIF4AI associated with ATP and RNA binding and ATP hydrolysis were first described using limited proteolysis [20]. Recombinant protein 6×His-eIF4AI [26] was subjected to limited proteolysis using trypsin in the presence of ATP, ADP, or poly(U) RNA in comparison with free enzyme (Figure 1A), and in the presence of combinations of AMP-PNP and poly(U) (precatalysis state) or ADP and poly(U) (postcatalysis state) (Figure 1B). The combination of AMP-PNP and poly(U) provided the most stable conformation with respect to trypsin susceptibility as indicated by the persistence of band A over time, implying a more closed structure, and poly(U) alone induced the most susceptible conformation. Band A (Figures 1 and 2; see below) was previously determined to arise from cleavage at Arg8 [20]. In all cases where the N-terminally tagged eIF4A was used, a cleavage occurred before the earliest time point assayed (4 min), giving a band corresponding to the same apparent molecular weight as band A previously described by Lorsch and Herschlag [20], likely indicating early removal of the N-terminal His tag. Precise cleavage points were not mapped in this study, as only global changes were under investigation. Nevertheless, bands at the apparent molecular weights that corresponded to bands described by Lorsch and Herschlag [20] were more than likely to have arisen from the same cleavage sites, due to the specificity of trypsin; thus, previously mapped cleavages (A, B/B′, and C) are indicated based on apparent molecular weight.

To assess effects of DMDA-PatA, limited proteolysis was performed on 6×His-eIF4AI alone or in the presence of individual substrates/products (Figures 1C–1F) with either DMSO (control), DMDA-PatA, or the inactive analog 90 [26] (control). No effects of DMDA-PatA were observed (no significant variation of banding patterns for DMDA-PatA-treated samples versus controls) for free 6×His-eIF4AI (Figure 1C) in the presence of saturating concentrations of ATP (Figure 1D) or for saturating ADP (Figure 1E). However, in the presence of saturating poly(U) RNA (Figure 1F), distinct differences in the cleavage profile were observed. Most significantly, the presence of DMDA-PatA destabilized the nearly full-length protein (band A), but stabilized an ~40 kDa (labeled X) fragment with respect to controls up to the 8 min time point (Figure 1F, lane 2 versus lanes 1 and 3, and lane 5 versus lanes 4 and 6). At the later time points, the DMDA-PatA-treated sample did not show the prominent ~30 kDa bands found in controls (Figure 1F, lane 8 versus lanes 7 and 9, and lane 11 versus lanes 10 and 12).

Next, DMDA-PatA effects on 6×His-eIF4AI were examined under saturating combinations of AMP-PNP and poly(U), or ADP and poly(U). In Figure 2A, the prominent ~30 kDa bands in controls were not present for DMDA-PatA treatment in the presence of AMP-PNP and poly(U) (e.g., Figure 2A, lane 8 versus lanes 7 and 9, and lane 11 versus lanes 10 and 12). Furthermore, a slight but reproducible stabilization of band A occurred in the presence of DMDA-PatA, which was more apparent for the untagged form of eIF4AI (see Figure S1A in the Supplemental Data available with this article online). Differences were also observed for the ADP and poly(U) combination, again with the appearance of band X that was observed for poly(U) only, which was also accompanied by loss of the ~35 kDa bands and the higher prominence of an ~25 kDa band (e.g., Figure 2B, lane 11 versus lanes 10 and 12). To examine for differences between AMP-PNP and ATP, the two compounds are directly compared in Figure 2C. Only one minor difference was observed at ~17.5 kDa, although this band was present for both samples, with stronger intensity for AMP-PNP. As results from assay to assay (gel to gel) cannot be directly compared due to variability in trypsin activity and reaction conditions, the three conditions where DMDA-PatA effects were observed, poly(U) alone, poly(U) and AMP-PNP, and poly(U) and ADP, were directly compared in Figure 2D. In this assay, stabilization of band A by DMDA-PatA was most prominent for the AMP-PNP and poly(U) combination (Figure 2D, lane 11 versus lanes 10 and 12), suggesting a more tightly closed or compact structure.

Substrate-Dependent Interactions of the Biotin-PatA Conjugate with eIF4AI

We have previously demonstrated the capability of B-PatA to capture 6×His-eIF4AI in buffer only [26]. However, these data required 6×His-eIF4AI to be in large molar excess to B-PatA. The lack of effect of limited proteolysis on 6×His-eIF4AI for free enzyme, or in the presence of nucleotide, could be interpreted in two ways with respect to the DMDA-PatA–eIF4AI interaction: (1) binding does not occur under these conditions and minimally requires the binding of RNA to eIF4AI before interaction may occur, or (2) binding of compound does occur, but structural changes are not induced or are not observable by limited proteolysis. To further define the requirement of poly(U) and AMP-PNP/ADP for the DMDA-PatA–eIF4AI interaction, capture

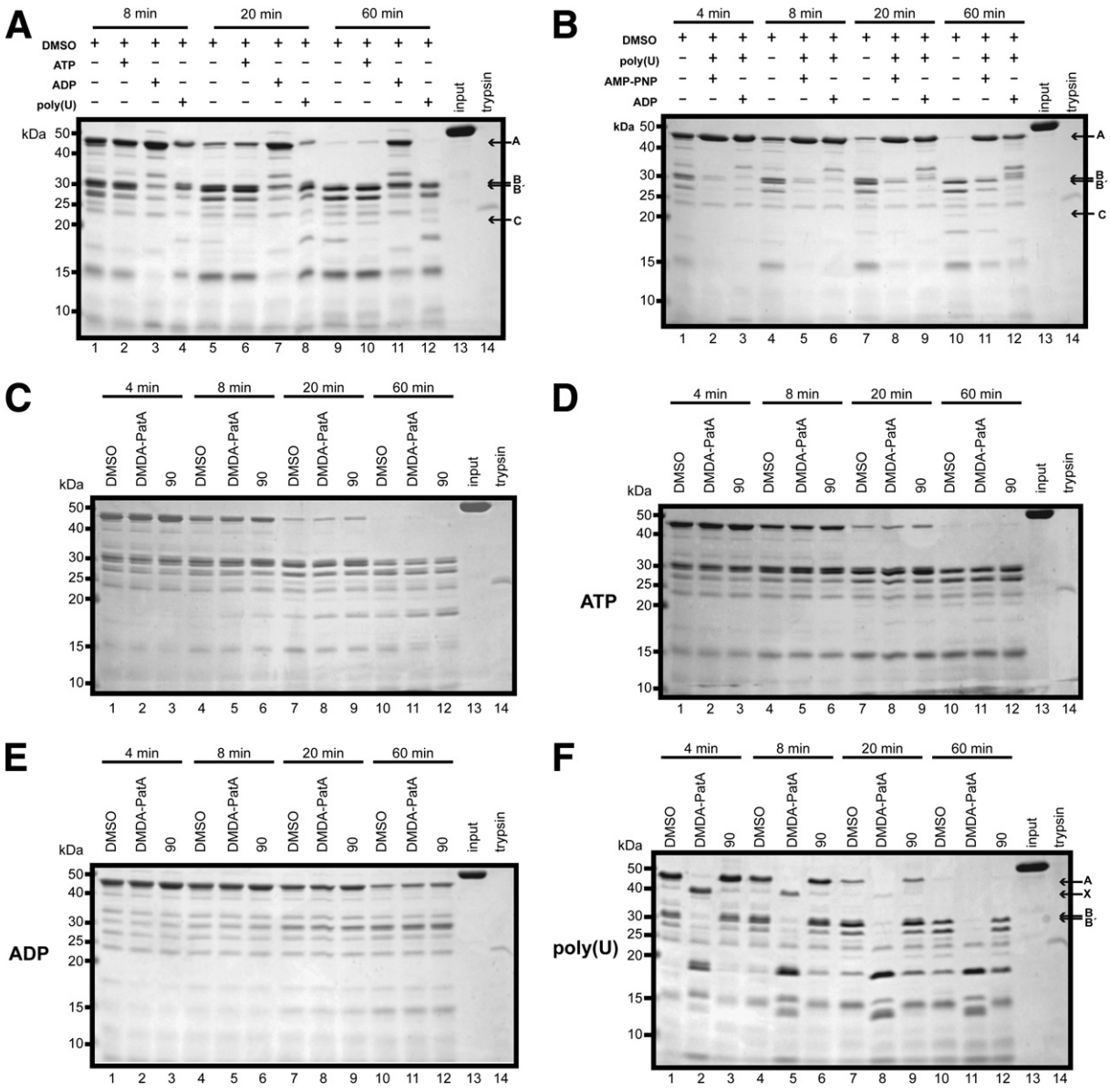

Figure 1. RNA-Dependent Conformational Change of eIF4AI Induced by DMDA-PatA

Time course of limited proteolysis analysis of 6×His-eIF4AI using trypsin. Input and trypsin lanes are amounts for 10 μl aliquots.

(A) Comparison of indicated individual substrates/products. All components are listed above the frames.

(B) Comparison of combined substrates, AMP-PNP and poly(U), and products, ADP and poly(U). All components are listed above the frames.

(C–F) Effects of DMDA-PatA on 6×His-eIF4AI conformation were compared with inactive analog 90 and DMSO in the presence of individual substrates/products. Additional components are listed to the left of each frame.

assays were performed using B-PatA and untagged eIF4AI. Furthermore, these assays were performed with eIF4AI in only 2-fold molar excess to B-PatA, in contrast to previous studies [26]. In Figure 3A, eIF4AI was efficiently captured by B-PatA in the presence of AMP-PNP and poly(U) RNA (Figure 3A, lane 6), which was effectively prevented by preincubation with DMDA-PatA as a competitor (Figure 3A, lane 7), but no interaction was detected in buffer alone (Figure 3A, lanes 2–4). Surprisingly, the presence of poly(U) did not enhance the capture of eIF4AI by B-PatA (Figure 3B, lanes 5–7). Furthermore, the presence of Mg^{2+}·AMP-PNP did not promote interaction, consistent with the limited proteolysis data (Figure 3C, lanes 5–7). Due to the length and nonuniformity of the poly(U) used (average of 160 nucleotides in length), the possibility of multiple eIF4AI proteins being captured by binding to the same poly(U) molecule was controlled for by comparison with an 11-mer RNA (Figure 3D). In this instance, both the 11-mer (R11) and poly(U) were capable of inducing capture of eIF4AI by B-PatA. The limited proteolysis data indicated

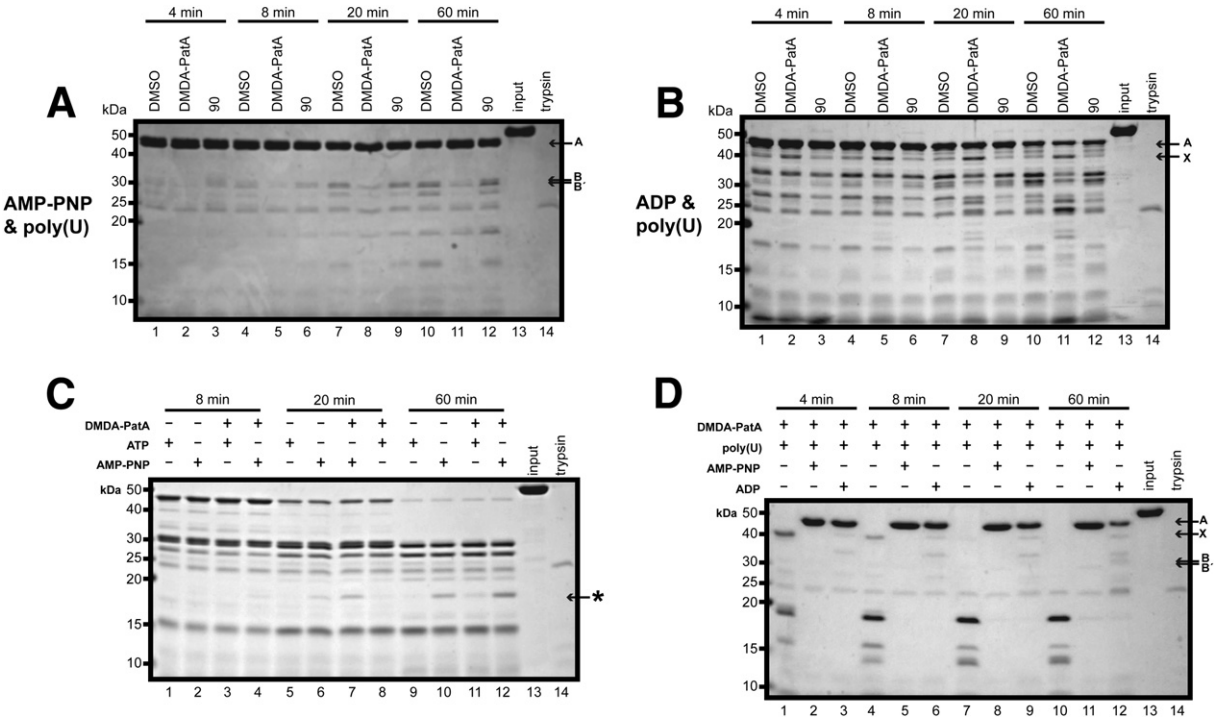

Figure 2. Proteolysis Stable Conformation of eIF4AI Induced by DMDA-PatA in the Combined Presence of Nonhydrolyzable ATP Analog and Poly(U)

Time course of limited proteolysis analysis of 6×His-eIF4AI using trypsin. Input and trypsin lanes are amounts for 10 μl aliquots.

(A and B) Additional components are listed to the left of each frame.

(C and D) All components are listed above each frame. Effects of DMDA-PatA on 6×His-eIF4AI conformation were compared with inactive analog 90 and DMSO in the presence of substrates/products.

(C) The asterisk indicates only observable difference.

(D) Direct comparison of three conditions, poly(U) only, poly(U) and AMP-PNP, and poly(U) and ADP, where effects were observed for DMDA-PatA.

that DMDA-PatA was capable of modulating the conformation in the presence of ADP and poly(U). Thus, this combination was also examined for B-PatA affinity (Figure 3E); however, ADP and poly(U) were unable to promote capture of eIF4AI (Figure 3E, lanes 2–4 versus lanes 5–7). Differences in substrate/product dependencies between limited proteolysis and B-PatA capture assays were not due to use of different forms of recombinant protein (His-tagged versus untagged), as the untagged protein responded similarly to limited proteolysis (Figure S1).

Activation of ATPase Activity for eIF4AI Homologs: tif1p and eIF4AIII

Due to the 90% sequence identity between eIF4AI and eIF4AII, the effects of PatA are likely to be similar for both proteins. Another homolog, eIF4AIII (DDX48), is also bound by PatA [28]. In yeast, two homologs to eIF4AI exist, tif1p and tif2p, which are identical in sequence and ~65% identical to eIF4AI. Recombinant forms of an N-terminally His-tagged eIF4AIII and untagged tif1p were examined for ATPase activity in the presence of DMDA-PatA. For both proteins, activation of ATPase activity was observed (Figures 4A and 4B). For 6×His-eIF4AIII, very little activity was detected in control (DMSO) assays, thus making accurate quantification of kinetic parameters and the increase in activity difficult; nevertheless, it is clear that both PatA and DMDA-PatA acted by increasing the turnover rate. For tif1p, DMDA-PatA increased both ATP affinity (as implied by a decrease in K_m) and increased turnover rate (k_{cat}). This is in contrast to previously reported results for 6×His-eIF4AI, where no significant increase of k_{cat} was observed [26].

Domain Linker-Dependent Activation of eIF4AI by DMDA-PatA

The ability to increase ATPase activity for eIF4AI(II), III, and tif1p, albeit with mechanistic differences with respect to kinetics, suggests that they share a common feature targeted by PatA. Accordingly, sequences for eIF4AI, II, III, and tif1p were aligned, and a second alignment with all known human DDX proteins [4] was performed, to identify commonalities among themselves and differences (for eIF4AI versus other human DDX proteins) that could be linked to PatA function (Figures S2 and S3). Previously, a minimal region of the N terminus of eIF4AI (residues 1–244) was found to be sufficient for capture by B-PatA [26]. Thus, focus was concentrated on this region. One outcome of this analysis was that all proteins that are activated by PatA have a strikingly similar domain linker of the sequence (D/N)P(I/V)RILVK(K/R)(E/D)ELTEG. Interestingly,

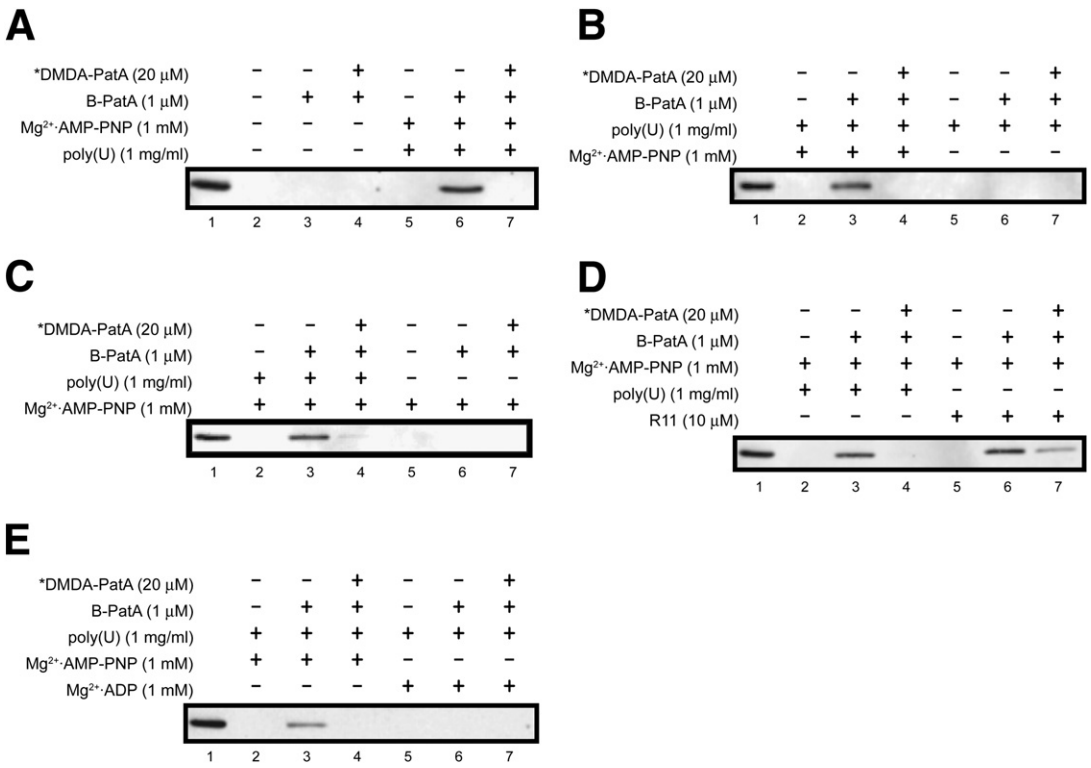

Figure 3. Substrate (AMP-PNP and RNA)-Dependent Interaction of Biotin-PatA with eIF4AI

(A–E) Lane 1 is 1% of total input. The asterisks indicate preincubation with free DMDA-PatA for 1 hr prior to addition of B-PatA. eIF4AI concentration is 2 μM.

(D) R11 refers to an 11-mer RNA with the sequence GCUUUACGGUG.

the K(K/R)(E/D)E region corresponds directly to the extended linker region of the tif1p crystal structure [18]. In the recently solved structures for the AMP-PNP- and RNA-bound forms of eIF4AIII (linker of KRDE) within the EJC, and of the *Drosophilia* DDX protein, Vasa (linker of GIVGG), the linker undergoes conformational changes to allow formation of the closed structure (see Discussion) [21–23]. Thus, site-directed mutagenesis was performed to determine any possible roles of the linker region in targeting of eIF4A by PatA.

Binding of residues 1–244 of eIF4AI by B-PatA [26] was confirmed using the recombinant protein eIF4AI(Δ246–406) at 2-fold molar excess to B-PatA in the presence of AMP-PNP and a 13-mer RNA molecule in a capture assay (Figure 5A). However, further removal of residues 237–245 (KKEELTLEG) in eIF4AI(Δ237–406) abrogated binding by B-PatA under identical conditions (Figure 5B). The KKEELTLE (residues 237–244) sequence of eIF4AI was then mutated to GKEELTLE, KKEGGTLE, GKEGGTLE, GKEGGTLA, or GAAGGTLE and recombinant proteins with N-terminal His tags, analogous to the previously described 6×His-eIF4AI [26], were produced and assayed for ATPase activity at saturating RNA and subsaturating (50 μM) Mg^{2+}·ATP concentrations. These conditions were chosen to maximize the observed effect of DMDA-PatA on the wild-type protein, as a ~2.5-fold increase in activity (saturating at 10 μM DMDA-PatA for wild-type; Figure 5C) was previously observed for wild-type [26]. The mutations were designed to gradually change the eIF4AI, II, and III sequence to more closely resemble that found in Vasa, which has a linker of the form GxxGG (Figure S3). In fact, the linker sequence Gxx(x/G) is more highly represented within the human DDX family (Figure S2).

Strikingly, the replacement of Lys237 with Gly (GKEELTLE) demonstrated a significant increase in ATPase activity in the absence of DMDA-PatA, and even greater increases in activity were observed when Glu240 and Leu241 (KKEGGTLE) were replaced with Gly (Figure 5D). However, for both proteins, DMDA-PatA was observed to further enhance activity. When the two mutations were combined in GKEGGLTE, DMDA-PatA was no longer able to increase ATPase activity, even when concentrations of DMDA-PatA were increased 5-fold. Similar results were observed for the GKEGGLTA and GAAGGLTE mutations. For all three mutants (GKEGGLTE, GKEGGLTA, and GAAGGLTE), activity levels were approximately equal to the level of activity for KKEGGLTE in the presence of DMSO. Thus, although replacement of Lys237 alone, or of Glu240 together with Leu241, increased activity in DMSO, the combination of both mutations (K237G and E240G with L241G) was not additive. To examine whether these domain-linker residues are involved in PatA binding,

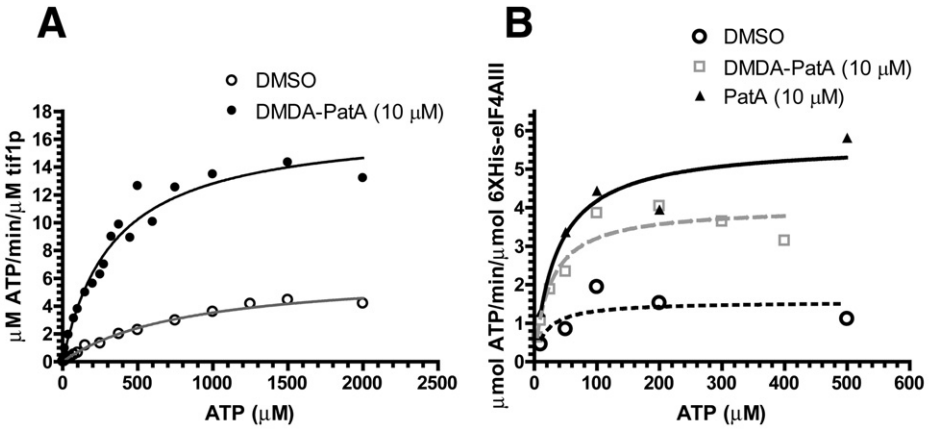

C

	K_m (μM)		k_{cat} (min^{-1})		k_{cat}/K_m ($M^{-1}\cdot s^{-1}$)	
	DMSO	DMDA-PatA	DMSO	DMDA-PatA	DMSO	DMDA-PatA
*6XHis-eIF4AI	107.6±30	34.7±4.5	3.4±0.4	4.55±0.2	5.3×10^2	22.0×10^2
tif1p	841±105	336.5±51	6.5±0.4	17.1±1.0	1.3×10^2	8.5×10^2
6XHis-eIF4AIII	18.9±24.3	25.6±9.1	1.6±0.4	4.0±0.33	14.0×10^2	26.0×10^2

Figure 4. Activation of ATPase Activity of eIF4AI Homologs tif1p and 6×His-eIF4AIII by PatA

(A) ATPase activity of recombinant tif1p in the presence of saturating RNA in the presence of control (DMSO) or 10 μM DMDA-PatA.

(B) ATPase activity of recombinant 6×His-eIF4AIII (N-terminally His-tagged) under saturating RNA concentrations in the presence of control (DMSO), 10 μM DMDA-PatA, or 10 μM PatA.

(C) Kinetic parameters derived from (A) and (B) after curve fitting. The asterisk indicates values determined in Low et al. [26].

B-PatA capture assays were performed for the GKEGGLTE, GKEGGLTA, and GAAGGLTE mutants (Figure 5E). However, all mutants were efficiently captured by B-PatA in the presence of AMP-PNP and poly(U).

The GKEGGTLE mutant was selected for further analysis by limited proteolysis (Figure 6). Similar to the wild-type protein, no differences were observed between DMDA-PatA treatment versus controls (DMSO or analog 90) over the time course of the assay when no substrates/products were added (Figure 6A). When poly(U) was included (Figure 6B), DMDA-PatA again stabilized band X versus controls up to the 8 min time point (Figure 6B, lane 2 versus lanes 1 and 3, and lane 5 versus lanes 4 and 6). For later time points, DMDA-PatA treatment showed loss of the prominent ~30 kDa bands found in controls (Figure 6B, lane 8 versus lanes 7 and 9, and lane 11 versus lanes 10 and 12). This response to DMDA-PatA was similar to wild-type protein under identical conditions (Figure 1F). However, when AMP-PNP was included along with poly(U) (Figure 6C), the DMDA-PatA-treated sample did not vary significantly in comparison to control samples (DMSO and analog 90) at all time points. This is in contrast to wild-type, where DMDA-PatA treatment demonstrated stabilizing effects over time with respect to trypsin in the presence of AMP-PNP and poly(U) (Figure 2A; Figure S1B). When AMP-PNP was replaced with ADP in cotreatment with poly(U), DMDA-PatA again displayed observable effects in comparison with controls (e.g., Figure 6D, lane 11 versus lanes 10 and 12), similar to wild-type protein (Figure 2B). When comparing poly(U) alone, versus poly(U) and AMP-PNP or poly(U) and ADP, the most stability with respect to trypsin digestion was again in the presence of AMP-PNP and poly(U), which was similar to wild-type (see Figure S7).

DISCUSSION

The marine natural product PatA and its close derivative DMDA-PatA inhibit eukaryotic cap-dependent translation initiation and increase both the ATPase and helicase activities of their target protein eIF4AI. Here, we demonstrate that strong binding of PatA to eIF4AI is dependent on the presence of eIF4AI substrates ATP and RNA. Furthermore, PatA promotes formation of the closed, more active conformation of eIF4AI, which is likely mediated by relief of the negative regulation provided by the linker sequence unique to eIF4AI(II) and the related homologs eIF4AIII and yeast tif1/2p (see Figures S2 and S3).

For all DDX proteins where structural information exists, a minimum two-domain structure consisting of the N-terminal domain which contains the Walker A and B motifs and a C-terminal domain necessary for activity has been observed. For eIF4A, the two domains must be brought into close proximity in the correct orientation to allow the energy of hydrolysis of ATP to be translated into the work of unwinding duplex RNA [18]. More recently, crystallographic studies of the core region of the *Drosophilia* DDX protein Vasa in complex with AMP-PNP and poly(U) have revealed the mechanism by which the nonprocessive helicase activity functions [23]. Conformational

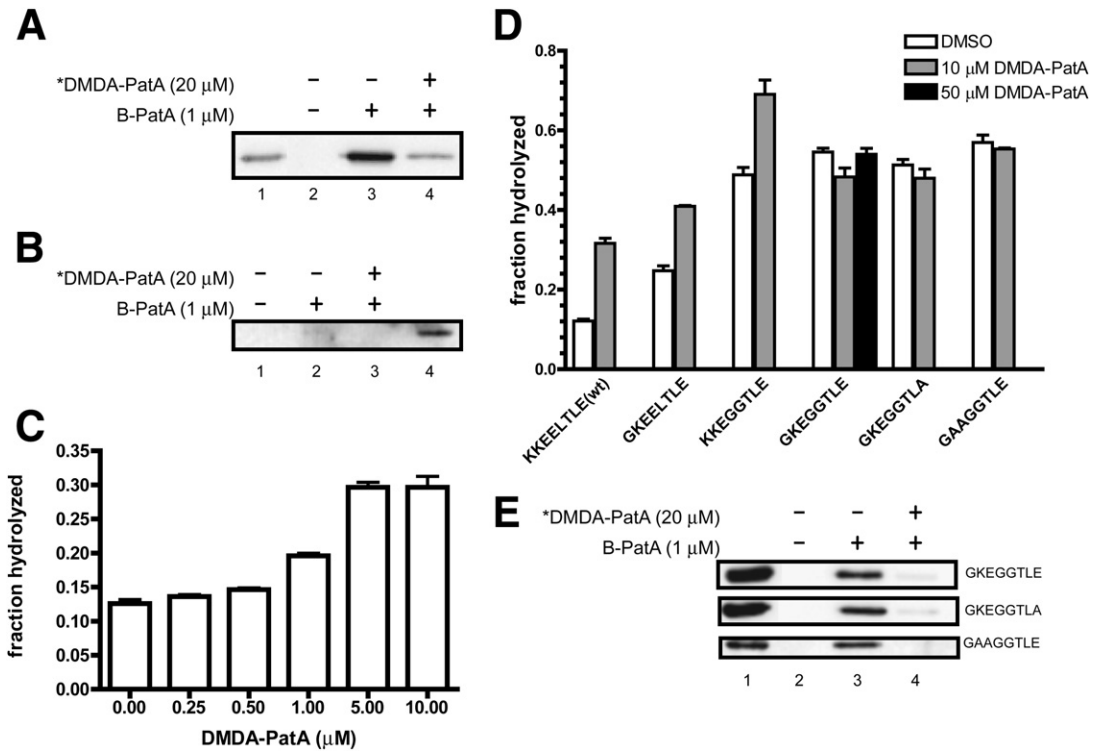

Figure 5. The Domain Linker of eIF4AI Is Involved in ATPase Enhancement Mediated by DMDA-PatA

(A and B) B-PatA capture assays for eIF4AI(Δ246–406) (A) or eIF4AI(Δ237–406) (B) in the presence of 1 mM Mg^{2+}·AMP-PNP and 10 μM 13-mer RNA oligo (UUGGGGGAUUGCA). Lanes 1 (A) and 4 (B) are 1% of total input.

(C) ATPase activity of 6×His-eIF4AI under saturating RNA concentrations and subsaturating ATP (50 μM) with increasing DMDA-PatA concentrations.

(D) ATPase activity of indicated proteins under the same conditions as (C) with indicated concentrations of DMDA-PatA.

(C and D) Measurements for each concentration were from a minimum of three independent assays, with error bars representing +1 SEM.

(E) B-PatA capture assays for indicated mutant proteins. Protein concentrations used were 2 μM with 2% of input in lane 1 for GKEGGLTE and GKEGGLTA, and 1% of input for GAAGGLTE. Capture assays contained 1 mM Mg^{2+}·AMP-PNP and 1 mg/ml poly(U) RNA.

The asterisks in (A), (B), and (E) indicate preincubation for 1 hr.

changes within the linker region were revealed that allowed for formation of a closed structure that created an interdomain cleft with AMP-PNP bound within the cleft and with RNA running perpendicular to the cleft [23]. Furthermore, the structure revealed that the RNA conformation was sharply bent due to steric clashing with helix α7, thereby disrupting nucleotide base stacking, which in turn would disrupt base pairing, thus leading to the partial unwinding of short duplexes [23]. This model was confirmed by crystallographic studies of the four exon junction proteins MLN51, Magoh, Y14, and eIF4AIII, where the same sharp bending of RNA caused by the "wedge" helix was observed [21, 22]. As such, it is not surprising that the increased activity in the presence of PatA was observed to be associated with a more closed conformation as revealed by the limited proteolysis experiments. What is interesting is the minimal requirement of RNA to allow this observation. Indeed, the closed conformation has been known to be induced by substrates for some time [19, 20]. Coupled with the need for both substrates for efficient capture by B-PatA, and previous results describing increased affinity for ATP and RNA in the presence of PatA [26, 28], these results may suggest that in the unbound or apo form of eIF4A and in the nucleotide-only bound state, the binding site of PatA does not exist. This interpretation would also be consistent with previous studies where increased ATP affinity was only observed in the presence of saturating RNA [26, 28] but no change in ATP cross-linking was observed in the absence of RNA [28]. Thus, binding of substrates (minimally RNA) is required to allow binding of PatA, which then strengthens the association for both RNA and ATP by stabilizing the closed conformation, thereby increasing enzymatic activity (see Figure 7).

Differences of substrate/product requirements for DMDA-PatA and B-PatA between the limited proteolysis and capture assays could suggest that the two PatA analogs interact with eIF4A by different mechanisms. While possible, this scenario is unlikely, as DMDA-PatA effectively competed with B-PatA for binding. Another possibility is that both analogs interact with eIF4A by the same mechanism, and the different substrate/product requirements are the consequence of lower binding affinity of B-PatA for eIF4A; that is, affinity of DMDA-PatA is high enough to only require RNA, whereas B-PatA also requires AMP-PNP to induce further changes in eIF4A to allow binding. This would also be in agreement with the lower

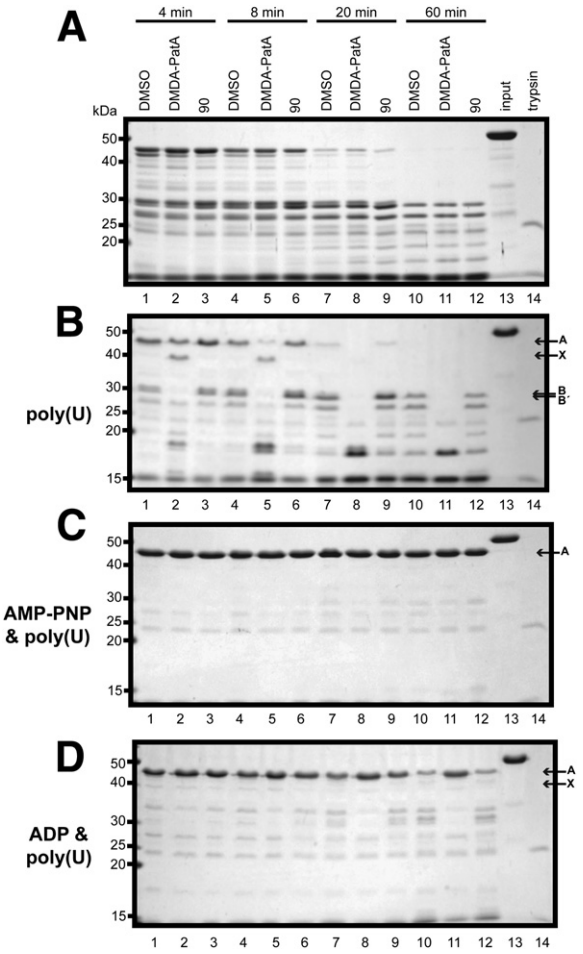

Figure 6. Mutation of Domain Linker Negates Effects of DMDA-PatA in the Presence of AMP-PNP and Poly(U)

Time course of limited proteolysis analysis of GKEGGTLE mutant (see text) using trypsin. Additional components are listed to the left of each frame. Labels above (A) apply to (A)–(D).

activity of B-PatA versus DMDA-PatA in cellular assays. This interpretation would suggest that the most tightly bound form or "state" of eIF4A by PatA is prior to catalysis (AMP-PNP and poly[U]). Interaction with the poly(U)-bound state may be weaker or transient in nature, which would also apply to the ADP and poly(U)-bound state. The inherent differences in conditions for the two assays should also be considered when making comparisons between results.

Previous studies where it was determined that binding of RNA was stronger in the presence of ATP or nonhydrolyzable analog but was drastically reduced in the presence of ADP or the slowly hydrolyzable analog ATPγS [19, 30, 31] should also be included in the analysis of results presented here. Given the fact that PatA required minimally the presence of RNA to exert structural changes, the presence of ADP within the capture assays may reduce RNA binding and, thus, B-PatA binding. However, association was enough to be detected in the limited proteolysis assays. The possibility that PatA may also be modulating the RNA affinity in the presence of ADP (i.e., increased RNA binding compared to control) should be considered as part of a putative activating mechanism. PatA may be allowing the hydrolysis of ATP to ADP without the obligatory release of RNA observed for eIF4A alone [19, 20]. Another intriguing possibility is that PatA binding may also cycle through binding and release along with RNA during the catalytic cycle, although there is no direct evidence to suggest this mechanism at this time. Furthermore, these results may suggest that binding of PatA requires functional groups from RNA itself as well as determinants found in eIF4A. One caveat to the use of limited proteolysis to gain structural information is that binding of PatA may not be changing global conformation, but may cause protection of cleavage sites from trypsin. Nevertheless, this would not change conclusions made concerning the PatA-eIF4A interaction, and more detailed and direct structural studies are still necessary.

Those proteins determined thus far to have increased activity in the presence of PatA share a common domain-linker sequence K(K/R)(E/D)E. Based on sequence alignment, another sequence commonly found in this region of human DDX proteins is Gxx(x/G) (see Figure S2). Comparison of the linker regions from the Vasa and the EJC structures [21–23] identifies two conformational changes in the linker region that facilitate the close proximity of the two domains (see Figure S4). In Vasa, the linker region "kinks" to bring the two domains together [23]. In the EJC structures [21, 22], the linker region (residues KRDE) adopts a helical structure to allow domain contact. For eIF4AIII, stabilizing contacts are made with the EJC proteins Magoh and Y14.

Although full characterizations of activity were not performed for the eIF4AI mutants, it is of interest that sequentially mutating the KKEEL linker to GKEEL, KKEGG, GKEGG, and GAAGG (Vasa equivalent) also increased ATPase activity even in the absence of PatA. These results may indicate that the conservation of the K(K/R)(E/D)E sequence in eIF4AI, II, and III may be related to a regulatory function designed to maintain the "inactive" conformation, which must be overcome to allow ATP hydrolysis. The nonadditive effects of the GKEELTLE and the KKEGGLTE mutations (Figure 5D), with the GKEGGTLE mutation having the same level of activity as the KKEGGLTE mutant (under DMSO), may suggest that the negative regulation is mediated by Glu240 and Leu241, with modulation by Lys237, and the lack of DMDA-PatA effects on ATPase activity only for GKEGGLTE suggests that PatA acts by altering function of all three residues.

Hydrolysis of ATP requires conserved residues from both domains, and although unbound forms of DDX proteins demonstrate variability in domain orientation [5], active forms likely involve very similar orientations. For eIF4A, the linker sequence may act to suppress aberrant domain interaction, and may require the binding of other regulatory proteins to overcome the linker sequence to allow the two domains to come into contact. This regulatory function of the linker may be negated in the presence of

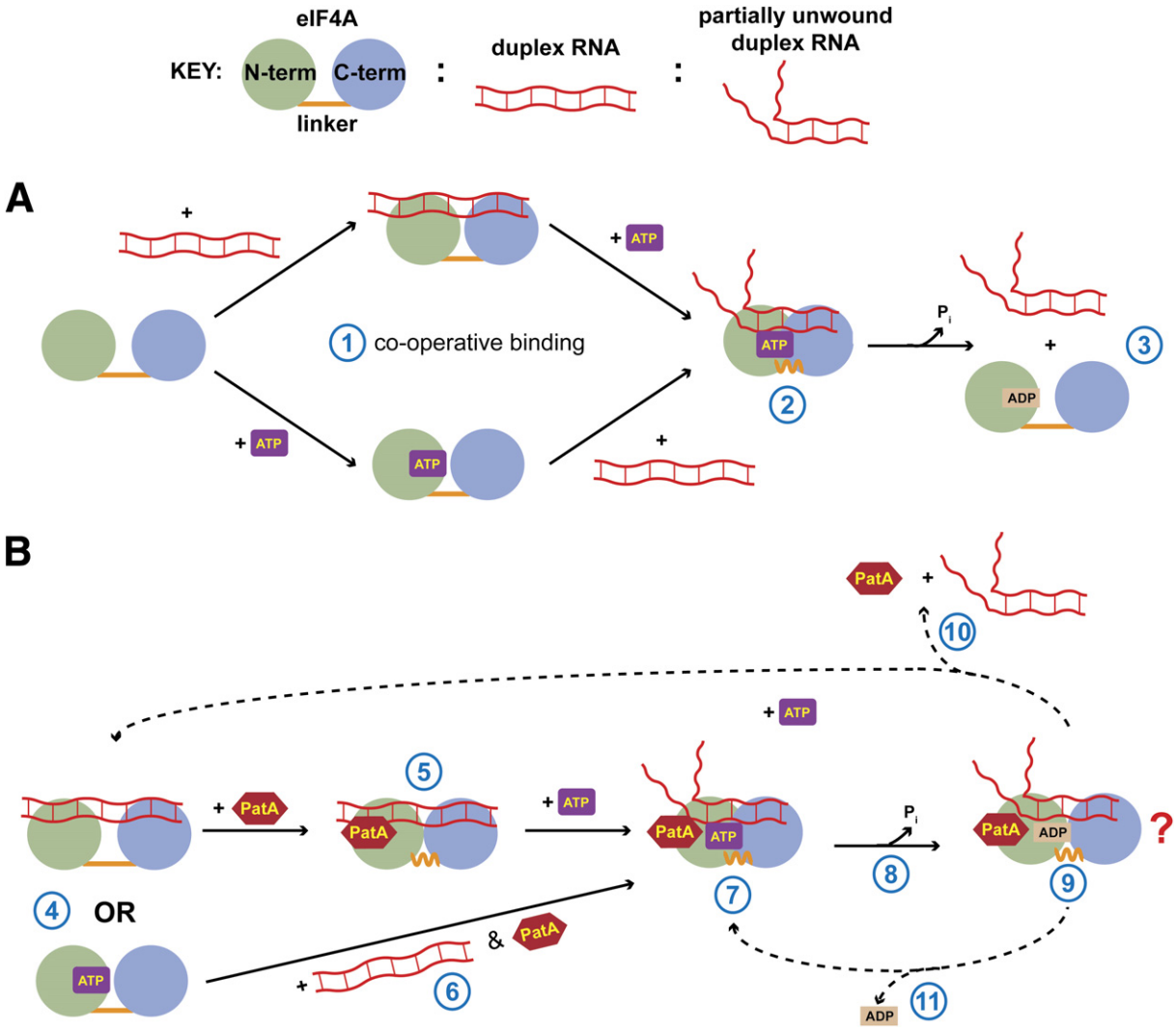

Figure 7. Schematic Representation of the Effects of PatA on eIF4A Conformation and Activity

(A) Cycle of ATP and RNA binding, ATP hydrolysis to ADP, and RNA release under normal conditions. (1) Cooperative binding of substrates, ATP, and duplex RNA [19, 20]. The linker prevents aberrant activity (or RNA interaction) by negatively regulating domain contact. (2) N- and C-terminal domains are prevented from close contact by the linker until both substrates are bound (which may also be regulated by other eIF4A binding proteins not shown). The linker undergoes a transition from an extended conformation to a more compact helix structure. The closed structure causes kinking and partial "unwinding" of duplex RNA [21–23]. (3) ATP is hydrolyzed to ADP, causing release of RNA. eIF4A returns to an "open" conformation. (B) Proposed mechanism(s) of deregulation and activation of eIF4A by PatA with respect to ATPase and helicase activity. (4) Binding of either RNA or ATP. (5) Limited proteolysis data suggest that minimally RNA is needed for PatA to interact with eIF4A. PatA increases affinity for ATP under saturating RNA concentrations, and increases RNA affinity under saturating ATP conditions [26, 28]. (6) If only ATP is bound, PatA requires RNA as well to bind to eIF4A. (7) Compact "closed" structure is formed by eIF4A, and further enhanced by PatA acting to remove negative effects of the linker toward ATPase activity. PatA may interact with both eIF4A and RNA. This "state" is likely the highest-affinity state for PatA binding, and may obviate the need for binding of "activating" proteins such as eIF4G. (8) Hydrolysis of ATP to ADP. (9) Limited proteolysis data suggest that this complex is altered in the presence of PatA. Consequences of PatA presence at this stage are unknown at this time. (10) If RNA is released, PatA may no longer bind to eIF4A, and a new cycle of binding and hydrolysis may occur, or (11) PatA may alter the obligatory release of RNA from eIF4A, and PatA and RNA may remain bound to eIF4A with only exchange of ADP for a new molecule of ATP.

PatA, and the increased activity is a consequence of allowing more accessibility to the closed conformation. Furthermore, the tight binding of B-PatA only in the presence AMP-PNP and RNA (Figure 3), and the lack of limited proteolysis effects for DMDA-PatA in comparison with controls on the GKEGGTLE mutant observed in the presence of AMP-PNP and poly(U) (Figure 6C), suggests that PatA specifically exerts its effects on the linker while eIF4A occupies the closed conformation during its catalytic cycle. The lack of increased activity for the GKEGGLTE and GAAGGLTE mutants when in the presence of DMDA-PatA, but the efficient capture of these mutants by B-PatA, suggests that when residues Lys237, Glu240, and Leu241 are mutated to Gly residues, binding of PatA is

inconsequential to ATPase activity. PatA may act by relieving inhibitory effects of these residues toward the stability of the closed structure, necessary for hydrolysis of ATP to ADP. This hypothesis also presupposes that the activation of ATPase activity by PatA does not grossly change the specific mechanism of hydrolysis.

Based on the aforementioned structures of the EJC and our previously reported results of changes in protein-protein interactions for eIF4AI in the presence of PatA [26], perturbation of the regulatory role of the linker region may be involved in the mechanism of translation inhibition caused by PatA-eIF4A binding. Thus, proteins that modulate eIF4A activity may act through modulation of the conformation of this linker region. However, the lack of binding by B-PatA for the eIF4AI(Δ237–406) protein would suggest that the linker is necessary for binding. These incongruent results may reflect unknown deleterious effects caused by deletion mutations. Another possible regulatory function of the linker region may be to prevent aberrant or spurious interaction with RNA (see below) based on the recently proposed mechanism of Bordeleau et al. [32].

Evidence to date suggests that eIF4AI may adopt several different states that are associated with differing levels of enzymatic activities, with each state having varying affinities for eIF4A's partner proteins, and that PatA may act by preferentially stabilizing a more active state, thus upsetting the natural balance and cycling of the states required for proper function [26, 28]. It has been suggested that for ribonucleoprotein (RNP) complexes, conformational changes in DDX proteins induced by the dissociation or binding of other subunits of the RNP complex may alter the position of the RNA substrate which allows activation of ATPase activity of the DDX protein, which in turn further alters the RNP complex [4]. Furthermore, activation of ATPase activity and hydrolysis of ATP to ADP may be associated with release of RNA substrate. These models suggest that the cycle of conformational changes, and the timing of ATP hydrolysis, is a tightly regulated process within the cellular milieu which is highly dependent on the DDX-associated proteins. Thus, the removal of the proposed regulatory role of the eIF4A linker sequence in the presence of PatA may lead to inhibition of translation initiation by disrupting the proper timing of events in translation initiation normally associated with the binding of various eIF4A binding proteins.

The RNA binding, ATPase, and helicase activities of eIF4A are all enhanced when it is incorporated into eIF4F, suggesting that binding to eIF4G activates eIF4A [16, 33–35]. Furthermore, the RNA binding proteins eIF4B and eIF4H have been reported to increase eIF4A and eIF4F activity [15, 35]. There are several isoforms and homologs of eIF4G, the largest and most abundant being eIF4GI, which possesses two eIF4A binding sites [2, 36–38]. The first binding site (middle domain) increases ATPase activity, whereas the second site (C-terminal domain) regulates activity [39]. Furthermore, eIF4G has been proposed to act as a ''soft clamp'' that stabilizes eIF4A in a closed active conformation [40]. Given the differing functions with regard to ATPase activity for the two eIF4A binding domains in eIF4G [39], with the middle domain increasing RNA affinity and the C-terminal domain decreasing RNA affinity at subsaturating ATP concentrations, the substrate dependencies for DMDA-PatA observed here may have implications with regard to regulation of eIF4A activity by the two eIF4G domains. It is also of note that the middle domain is sufficient to allow translation initiation, with eIF4A implicated as a critical binding partner [41, 42]. Taking into account the decreased eIF4GI, and increased eIF4B association of eIF4AI in the presence of PatA [26], an analogous role to the accessory proteins of eIF4AIII in the EJC may be played by eIF4G, eIF4B, and eIF4H for eIF4AI, and PatA may be interfering with these proteins, leading to downstream effects causing translation initiation inhibition.

It has been previously suggested that PatA is unlikely to target eIF4A already present in the eIF4F complex, which was based on the observation that PatA did not change the RNA or ATP binding properties of eIF4F in crosslinking assays [28]. The decreased incorporation of eIF4A into the eIF4F complex in the presence of PatA or DMDA-PatA [26, 32] suggests that the eIF4A-PatA complex may be blocked from associating with eIF4G, thereby inhibiting the proper function of eIF4F. Based on more recent results [32], a mechanism has been proposed whereby free eIF4A is sequestered on RNA by PatA in a sequence-independent manner, thereby leading to decreased amounts of eIF4A available for formation of eIF4F, causing loss of 43S recruitment to mRNA [32]. This is slightly different from our previously proposed mechanism, whereby PatA causes changes in eIF4A's inherent protein-protein interactions leading to stalling of the 48S complex [26]. In light of the proposed substrate-dependent targeting of eIF4A by PatA presented here, both models should be reevaluated. What has remained consistent is that the presence of PatA seems to affect the eIF4F complex through direct targeting of eIF4A, whether by actively dissociating eIF4A from eIF4F or by preventing eIF4A incorporation into eIF4F, thus disrupting its normal function in translation initiation. Clearly, a deeper understanding not only of PatA but eIF4A function as well is needed before a more accurate mechanism of PatA inhibition of translation initiation can be postulated.

SIGNIFICANCE

Eukaryotic cap-dependent translation initiation is a complex process that involves the proper function of a number of proteins, several of which are points of regulation. One of the key protein complexes involved in translation initiation is eIF4F. The eIF4A component of eIF4F is thought to be critical for the translation initiation because of its ability to unwind local secondary structure allowing binding of the 43S ribosomal complex. Rapid cell proliferation associated with various types of cancers is often accompanied by deregulated protein translation [43, 44]. Furthermore, eIF4AI itself was found to be overexpressed in several melanoma cell lines, with downregulation of eIF4AI by antisense RNA leading to decreased proliferation rates [45, 46].

Targeting of eIF4A by the natural product pateamine A leads to an inhibition of cap-dependent translation, making PatA and its derivatives attractive candidates for further development as potential therapeutics. Here we have gained further insight into the PatA mechanism of inhibiting translation initiation by demonstrating that the PatA derivative DMDA-PatA deregulates the cycle of conformational changes in eIF4A associated with hydrolysis of ATP. Furthermore, we have demonstrated that this functional effect is dependent on an eIF4AI, II, and III unique sequence within the domain-linker region. This domain-linker region is proposed to negatively regulate eIF4A activity by preventing anomalous formation of the active closed conformation. A preliminary model is proposed where the negative regulation of the linker is relieved by association of eIF4A with its cognate protein binding partners under normal conditions, and the presence of PatA disrupts this cycle of protein-protein interactions by negating the need for binding proteins to activate eIF4A.

EXPERIMENTAL PROCEDURES

Recombinant Proteins

All recombinant proteins were produced by expression in *Escherichia coli* BL21(DE3) cells (Novagen) by induction with IPTG. After growth and harvesting, cells were lysed in lysis buffer by sonication. For His-tagged proteins, purification was performed using Ni-NTA resin (QIAGEN) at room temperature. For untagged proteins, purification involved anion-exchange chromatography using DEAE Sepharose (GE Healthcare) using a KCl gradient, followed by purification using a phosphate gradient on a hydroxylapatite column (Bio-Rad). All purification of untagged proteins was carried out at 4°C. After purification, all proteins were stored in buffer containing 20 mM Tris (pH 7.4), 100 mM KCl, 0.1 mM EDTA, 2 mM DTT, and 10% glycerol (eIF4A storage buffer), unless otherwise indicated. Protein concentrations were determined by OD_{280nm} and protein purity was monitored by SDS-PAGE and Coomassie blue staining (Figure S5). Detailed protocols for purification of each protein are provided in Supplemental Data.

Limited Proteolysis

Limited proteolysis was performed essentially as described in [20] using sequencing-grade trypsin (Roche Diagnostics). For 6×His-eIF4AI, reactions were performed at room temperature in 50 μl volumes using 0.2 mg/ml His-eIF4AI and 40 ng/ml trypsin. Buffer components were 20 mM Tris (pH 7.4), 80 mM KCl, 2.5 mM $MgCl_2$, 1 mM DTT, and 1% glycerol. DMSO was present at 5% of reaction volume either as a control or compound solvent. Ten microliter aliquots were collected at indicated time points and trypsin activity was quenched by heating in 2× SDS-PAGE sample loading buffer containing 100 mM KOH. Mg^{2+}·ATP, ·ADP, and ·AMP-PNP were at 5 mM, poly(U) was 3.75 mg/ml, and compounds were at 1 mM. For untagged eIF4AI, reaction conditions were identical using 0.2 mg/ml eIF4AI. Proteolysis products were visualized by SDS-PAGE and Coomassie blue staining.

Biotin-PatA Capture Assays

B-PatA pull-downs were performed as described in [26]. eIF4AI, 6×His-eIF4AI, or eIF4AI mutations were premixed in buffer containing 20 mM Tris (pH 7.4), 100 mM KCl, and 0.2% Triton-X-100, then divided into equal aliquots. Indicated components were added and final pull-down volumes of 200 μl were used containing 5 mg/ml BSA. B-PatA was captured using streptavidin-conjugated agarose (Pierce) pre-washed with 5 mg/ml BSA in buffer. Binding was performed at 4°C with a preincubation time of 1 hr (DMDA-PatA), binding time of 1 hr (B-PatA), and capture time of 1 hr (streptavidin-agarose), followed by three 5 min washes with 1 ml of buffer. Captured proteins were released by boiling of streptavidin-agarose in SDS-PAGE loading buffer followed by SDS-PAGE, transfer to nitrocellulose membranes, and visualization by immunoblotting using eIF4AI-specific or His tag-specific antibodies (Santa Cruz).

ATPase Assays

ATPase assays were performed as previously described in [39] with modifications described in [26]. Protein concentrations used were 0.7 μM for tif1p and 0.6 μM for 6×His-eIF4AIII with a poly(U) concentration of 3.75 mg/ml. Doubling of poly(U) concentration did not have any effect on activity, and reactions times were 10 min, which were within the linear range. For analysis of 6×His-eIF4AI mutants, assays were performed identically to that described in [26], with protein concentrations of 0.5 μM and an ATP concentration of 50 μM for 10 min at 37°C with 3.75 mg/ml poly(U), previously determined to be saturating for 6×His-eIF4AI [26].

Supplemental Data

Supplemental Data include seven figures, one table, and Supplemental Experimental Procedures and are available at http://www.chembiol.com/cgi/content/full/14/6/715/DC1/.

ACKNOWLEDGMENTS

This work was funded by the National Cancer Institute, the Keck Center, the Flight Attendant Medical Research Institute Fund (J.O.L.), the National Institutes of General Medical Sciences (D.R.), and a Canadian Institutes of Health Research Fellowship (W.-K.L.). The authors would also like to thank Dr. Jon Lorsch for provision of materials and helpful discussions, Dr. Sandra Gabelli for critical reading of the manuscript, and Dr. Jing Xu for assistance with preparation of the manuscript.

Received: January 27, 2007
Revised: May 7, 2007
Accepted: May 21, 2007
Published: June 22, 2007

REFERENCES

1. Silverman, E., Edwalds-Gilbert, G., and Lin, R.J. (2003). DExD/H-box proteins and their partners: helping RNA helicases unwind. Gene *312*, 1–16.
2. Cordin, O., Banroques, J., Tanner, N.K., and Linder, P. (2006). The DEAD-box protein family of RNA helicases. Gene *367*, 17–37.
3. Abdelhaleem, M., Maltais, L., and Wain, H. (2003). The human DDX and DHX gene families of putative RNA helicases. Genomics *81*, 618–622.
4. Linder, P. (2006). Dead-box proteins: a family affair—active and passive players in RNP-remodeling. Nucleic Acids Res. *34*, 4168–4180.
5. Caruthers, J.M., and McKay, D.B. (2002). Helicase structure and mechanism. Curr. Opin. Struct. Biol. *12*, 123–133.
6. Rogers, G.W., Jr., Komar, A.A., and Merrick, W.C. (2002). eIF4A: the godfather of the DEAD box helicases. Prog. Nucleic Acid Res. Mol. Biol. *72*, 307–331.
7. Hernandez, G., and Vazquez-Pianzola, P. (2005). Functional diversity of the eukaryotic translation initiation factors belonging to eIF4 families. Mech. Dev. *122*, 865–876.
8. Kapp, L.D., and Lorsch, J.R. (2004). The molecular mechanics of eukaryotic translation. Annu. Rev. Biochem. *73*, 657–704.
9. Merrick, W.C. (2004). Cap-dependent and cap-independent translation in eukaryotic systems. Gene *332*, 1–11.

10. Tange, T.O., Nott, A., and Moore, M.J. (2004). The ever-increasing complexities of the exon junction complex. Curr. Opin. Cell Biol. *16*, 279–284.

11. Pause, A., Methot, N., Svitkin, Y., Merrick, W.C., and Sonenberg, N. (1994). Dominant negative mutants of mammalian translation initiation factor eIF-4A define a critical role for eIF-4F in cap-dependent and cap-independent initiation of translation. EMBO J. *13*, 1205–1215.

12. Prevot, D., Darlix, J.L., and Ohlmann, T. (2003). Conducting the initiation of protein synthesis: the role of eIF4G. Biol. Cell. *95*, 141–156.

13. Svitkin, Y.V., Pause, A., Haghighat, A., Pyronnet, S., Witherell, G., Belsham, G.J., and Sonenberg, N. (2001). The requirement for eukaryotic initiation factor 4A (eIF4A) in translation is in direct proportion to the degree of mRNA 5′ secondary structure. RNA *7*, 382–394.

14. Pause, A., and Sonenberg, N. (1992). Mutational analysis of a DEAD box RNA helicase: the mammalian translation initiation factor eIF-4A. EMBO J. *11*, 2643–2654.

15. Rogers, G.W., Jr., Richter, N.J., Lima, W.F., and Merrick, W.C. (2001). Modulation of the helicase activity of eIF4A by eIF4B, eIF4H, and eIF4F. J. Biol. Chem. *276*, 30914–30922.

16. Grifo, J.A., Abramson, R.D., Satler, C.A., and Merrick, W.C. (1984). RNA-stimulated ATPase activity of eukaryotic initiation factors. J. Biol. Chem. *259*, 8648–8654.

17. Yoder-Hill, J., Pause, A., Sonenberg, N., and Merrick, W.C. (1993). The p46 subunit of eukaryotic initiation factor (eIF)-4F exchanges with eIF-4A. J. Biol. Chem. *268*, 5566–5573.

18. Caruthers, J.M., Johnson, E.R., and McKay, D.B. (2000). Crystal structure of yeast initiation factor 4A, a DEAD-box RNA helicase. Proc. Natl. Acad. Sci. USA *97*, 13080–13085.

19. Lorsch, J.R., and Herschlag, D. (1998). The DEAD box protein eIF4A. 1. A minimal kinetic and thermodynamic framework reveals coupled binding of RNA and nucleotide. Biochemistry *37*, 2180–2193.

20. Lorsch, J.R., and Herschlag, D. (1998). The DEAD box protein eIF4A. 2. A cycle of nucleotide and RNA-dependent conformational changes. Biochemistry *37*, 2194–2206.

21. Bono, F., Ebert, J., Lorentzen, E., and Conti, E. (2006). The crystal structure of the exon junction complex reveals how it maintains a stable grip on mRNA. Cell *126*, 713–725.

22. Andersen, C.B., Ballut, L., Johansen, J.S., Chamieh, H., Nielsen, K.H., Oliveira, C.L., Pedersen, J.S., Seraphin, B., Le Hir, H., and Andersen, G.R. (2006). Structure of the exon junction core complex with a trapped DEAD-box ATPase bound to RNA. Science *313*, 1968–1972.

23. Sengoku, T., Nureki, O., Nakamura, A., Kobayashi, S., and Yokoyama, S. (2006). Structural basis for RNA unwinding by the DEAD-box protein *Drosophila* Vasa. Cell *125*, 287–300.

24. Northcote, P.T., Blunt, J.W., and Munro, M.H.G. (1991). Pateamine: a potent cytotoxin from the New Zealand marine sponge, *Mycale* Sp. Tetrahedron Lett. *32*, 6411–6414.

25. Mazroui, R., Sukarieh, R., Bordeleau, M.E., Kaufman, R.J., Northcote, P., Tanaka, J., Gallouzi, I., and Pelletier, J. (2006). Inhibition of ribosome recruitment induces stress granule formation independently of eukaryotic initiation factor 2α phosphorylation. Mol. Biol. Cell *17*, 4212–4219.

26. Low, W.K., Dang, Y., Schneider-Poetsch, T., Shi, Z., Choi, N.S., Merrick, W.C., Romo, D., and Liu, J.O. (2005). Inhibition of eukaryotic translation initiation by the marine natural product pateamine A. Mol. Cell *20*, 709–722.

27. Dang, Y., Kedersha, N., Low, W.K., Romo, D., Gorospe, M., Kaufman, R., Anderson, P., and Liu, J.O. (2006). Eukaryotic initiation factor 2α-independent pathway of stress granule induction by the natural product pateamine A. J. Biol. Chem. *281*, 32870–32878.

28. Bordeleau, M.E., Matthews, J., Wojnar, J.M., Lindqvist, L., Novac, O., Jankowsky, E., Sonenberg, N., Northcote, P., Teesdale-Spittle, P., and Pelletier, J. (2005). Stimulation of mammalian translation initiation factor eIF4A activity by a small molecule inhibitor of eukaryotic translation. Proc. Natl. Acad. Sci. USA *102*, 10460–10465.

29. Romo, D., Choi, N.S., Li, S., Buchler, I., Shi, Z., and Liu, J.O. (2004). Evidence for separate binding and scaffolding domains in the immunosuppressive and antitumor marine natural product, pateamine A: design, synthesis, and activity studies leading to a potent simplified derivative. J. Am. Chem. Soc. *126*, 10582–10588.

30. Peck, M.L., and Herschlag, D. (2003). Adenosine 5′-O-(3-thio)-triphosphate (ATPγS) is a substrate for the nucleotide hydrolysis and RNA unwinding activities of eukaryotic translation initiation factor eIF4A. RNA *9*, 1180–1187.

31. Cordin, O., Tanner, N.K., Doere, M., Linder, P., and Banroques, J. (2004). The newly discovered Q motif of DEAD-box RNA helicases regulates RNA-binding and helicase activity. EMBO J. *23*, 2478–2487.

32. Bordeleau, M.E., Cencic, R., Lindqvist, L., Oberer, M., Northcote, P., Wagner, G., and Pelletier, J. (2006). RNA-mediated sequestration of the RNA helicase eIF4A by pateamine A inhibits translation initiation. Chem. Biol. *13*, 1287–1295.

33. Abramson, R.D., Dever, T.E., Lawson, T.G., Ray, B.K., Thach, R.E., and Merrick, W.C. (1987). The ATP-dependent interaction of eukaryotic initiation factors with mRNA. J. Biol. Chem. *262*, 3826–3832.

34. Abramson, R.D., Dever, T.E., and Merrick, W.C. (1988). Biochemical evidence supporting a mechanism for cap-independent and internal initiation of eukaryotic mRNA. J. Biol. Chem. *263*, 6016–6019.

35. Rozen, F., Edery, I., Meerovitch, K., Dever, T.E., Merrick, W.C., and Sonenberg, N. (1990). Bidirectional RNA helicase activity of eucaryotic translation initiation factors 4A and 4F. Mol. Cell. Biol. *10*, 1134–1144.

36. Bradley, C.A., Padovan, J.C., Thompson, T.L., Benoit, C.A., Chait, B.T., and Rhoads, R.E. (2002). Mass spectrometric analysis of the N terminus of translational initiation factor eIF4G-1 reveals novel isoforms. J. Biol. Chem. *277*, 12559–12571.

37. Coldwell, M.J., and Morley, S.J. (2006). Specific isoforms of translation initiation factor 4GI show differences in translational activity. Mol. Cell. Biol. *26*, 8448–8460.

38. Imataka, H., and Sonenberg, N. (1997). Human eukaryotic translation initiation factor 4G (eIF4G) possesses two separate and independent binding sites for eIF4A. Mol. Cell. Biol. *17*, 6940–6947.

39. Korneeva, N.L., First, E.A., Benoit, C.A., and Rhoads, R.E. (2005). Interaction between the NH_2-terminal domain of eIF4A and the central domain of eIF4G modulates RNA-stimulated ATPase activity. J. Biol. Chem. *280*, 1872–1881.

40. Oberer, M., Marintchev, A., and Wagner, G. (2005). Structural basis for the enhancement of eIF4A helicase activity by eIF4G. Genes Dev. *19*, 2212–2223.

41. De Gregorio, E., Preiss, T., and Hentze, M.W. (1998). Translational activation of uncapped mRNAs by the central part of human eIF4G is 5′ end-dependent. RNA *4*, 828–836.

42. De Gregorio, E., Preiss, T., and Hentze, M.W. (1999). Translation driven by an eIF4G core domain in vivo. EMBO J. *18*, 4865–4874.

43. Petroulakis, E., Mamane, Y., Le Bacquer, O., Shahbazian, D., and Sonenberg, N. (2006). mTOR signaling: implications for cancer and anticancer therapy. Br. J. Cancer *94*, 195–199.

44. Mamane, Y., Petroulakis, E., LeBacquer, O., and Sonenberg, N. (2006). mTOR, translation initiation and cancer. Oncogene *25*, 6416–6422.

45. Eberle, J., Krasagakis, K., and Orfanos, C.E. (1997). Translation initiation factor eIF-4A1 mRNA is consistently overexpressed in human melanoma cells in vitro. Int. J. Cancer *71*, 396–401.

46. Eberle, J., Fecker, L.F., Bittner, J.U., Orfanos, C.E., and Geilen, C.C. (2002). Decreased proliferation of human melanoma cell lines caused by antisense RNA against translation factor eIF-4A1. Br. J. Cancer *86*, 1957–1962.

